Optofluidics based membrane microreactor for wastewater treatment by photocatalytic ozonation

Xuefeng He[a,b], Rong Chen[a,b]*, Xun Zhu[a,b]**, Qiang Liao[a,b], Liang An[c], Xiao Cheng[a,b], Lin Li[a,b]

[a] Key Laboratory of Low-grade Energy Utilization Technologies and Systems (Chongqing University), Ministry of Education, Chongqing 400030, China

[b] Institute of Engineering Thermophysics, Chongqing University, Chongqing 400030, China

[c] Department of Mechanical Engineering, The Hong Kong Polytechnic University, Hung Hom, Kowloon, Hong Kong, China

*Corresponding author. Tel.: 0086-23-65102474; fax: 0086-23-65102474; e-mail: rchen@cqu.edu.cn

**Co-corresponding author. Tel.: 0086-23-65102474; fax: 0086-23-65102474; e-mail: zhuxun@cqu.edu.cn

Abstract

Conventional photocatalytic ozonation usually suffers from the mass transport issue associated with low specific surface area and gas/liquid interface and liquid film. To address this issue, a new membrane microreactor based on optofluidics was developed for wastewater treatment by the photocatalytic ozonation in this work. The key component of the photocatalytic membrane was prepared by coating TiO_2 onto carbon paper followed by the hydrophobic treatment with poly-tetrafluoroethylene. Such design offered several advantages of large surface-area-to-volume ratio, enhanced mass transport, intense and uniform light irradiation, efficient separation of the liquid/gas phases and good gas permeability. The performance of the developed microreactor was evaluated by the methylene blue degradation and products were analyzed by the ion chromatography. Experimental results showed that because of these advantages, the optofluidic membrane microreactor not only yielded better performance but also showed more complete oxidation as compared to the photocatalysis and ozonation. Parametric studies indicated that increasing the

residence time and decreasing the methylene blue concentration could improve the degradation efficiency. High light intensity benefited for the photocatalytic ozonation. The obtained results demonstrate the developed optofluidic membrane microreactor is feasible for wastewater treatment by the photocatalytic ozonation. Besides, this new type of microreactor can also be applied to other photocatalytic systems.

Keywords: optofluidic membrane microreactor; TiO_2/carbon paper composite photocatalytic membrane; photocatalytic ozonation; degradation efficiency

1. Introduction

With the rapid industrialization, water pollution has become a global issue. In particular, each year a significant amount of dye wastewater from textile industries is disposed into natural water resources, which threatens the human life and ecosystem. Therefore, to remove the organic compounds contained in the wastewater, various methods have been developed, such as physical adsorption, biodegradation and chemical oxidation and so on [1-3]. However, these methods cannot efficiently degrade the organic compounds contained in the colored wastewater due to the complicated composition, high COD and inconstant pH value [4-5]. For this reason, photocatalysis that is one of the advanced oxidation technologies, has been widely used for wastewater treatment because it can offer the advantages of strong oxidizing ability, high reaction rate and non-selective degrading ability to various organic compounds [6-7]. Over the past decades, hence, extensive efforts have been devoted to the study on the photocatalytic wastewater treatment [8-10].

In the photocatalytic wastewater treatment, the semiconductor of TiO_2 is typically used because of its low cost and high stability [11-12]. However, since TiO_2 can only well respond to the UV light, other semiconductors, such as ZnO, WO_3, CdS and their impregnated forms [13-16], have been developed to enable the visible-light response. Moreover, a new advanced oxidation method has also been developed by adding the oxidizing gases of oxygen, ozone or their mixture into the photocatalytic systems, represented by the photocatalytic ozonation [17-18]. It has been revealed that such combination can dramatically increase the amount of the oxidizing reagents and provide the synergistic effect to improve the degradation performance. Usually, in the photocatalytic ozonation process, the oxidizing gases are directly pumped into the

reactors along with the wastewater, forming the two-phase flow in the reactors [19-20]. Such operation mode brings two critical issues. First, the dissolvability of the oxidizing gas is small. Moreover, the oxidizing gases need to transport from the gas phase to the photocatalyst surface via the gas/liquid interface and liquid phase. In this case, the concentrations of the oxidizing reagents become low, limiting the improvement in the degradation performance. Second, the gas/liquid interfaces of the gas bubbles obstruct the incident light because of the reflection and scattering [21-22], which also weakens the photon transfer and thus lowers the performance. Fortunately, these two problems can be addressed by the membrane technology, which enables the separation of the gas phase from the liquid phase. As such, gas reactants can directly penetrate through the membrane, eliminating the mass transfer resistances associated with the gas/liquid interface and liquid phase. Besides, efficient photon transfer can also be enabled without the interference of gas bubbles. Therefore, the incorporation of the membrane technology is promising to promote the photocatalytic ozonation.

In addition, poor mass and photon transfer efficiencies are usually encountered in existing large-scale photocatalytic ozonation systems, which also limits the further improvement in the degradation performance. Recently, the combination of optics with microfluidics in the same platform leads to an emergent technology of optofluidics. Such synergy offers several merits inheriting from both optics and microfluidics, including high surface-area-to-volume ratio, fine flow control, efficient mass and proton transfer, intense and uniform light distribution, accurate controllability and high tunability. Clearly, the photocatalytic ozonation is also a typical optofluidic system since it shares the same features with optofluidics: light, fluids and their interactions [23-24]. Hence, optofluidics has shown promising

perspective for the photocatalytic wastewater treatment. Several optofluidic microreactors have been developed to enhance the degradation performance [25-29]. For example, Li et al. [28] developed an optofluidic microreactor with TiO_2-coated fiberglass for the wastewater treatment and found that this new microreactor showed a 2-3 fold improvement in the reaction rate constant. Lei et al. [29] developed the optofluidic planar reactors for photocatalytic water treatment using solar energy and found that the photoreaction efficiency was improved by more than 100 times.

The above literature review indicates that the photocatalytic ozonation, membrane technology and optofluidics have their respective intrinsic advantages towards the photocatalytic wastewater treatment. Although it has been demonstrated that the porous photocatalytic membrane microreactor can greatly improve the degradation efficiency due to sufficient supply of oxygen [30], the combination of the photocatalytic ozonation, membrane technology and optofluidics has not yet been reported. In this study, therefore, we developed an optofluidic membrane microreactor with a TiO_2/carbon paper composite photocatalytic membrane for wastewater treatment by the photocatalytic ozonation. The photocatalytic membrane was formed by coating TiO_2 onto carbon paper followed by the hydrophobic treatment with poly-tetrafluoroethylene (PTFE). The performance of the developed microreactor was then evaluated by degrading methylene blue under UV irradiance.

2. Experimental

2.1 Preparation of the TiO_2/carbon paper composite photocatalytic membrane

In this work, the photocatalytic membrane is the key component to form such an optofluidic membrane microreactor, which has to meet the following requirements: (i)

stable substrate for supporting the photocatalysts, (ii) efficient separation of gas/liquid phases, and (iii) good gas permeability. To this end, we proposed the TiO_2/carbon paper composite photocatalytic membrane. Unlike the work by Aran et al. [30], in which the porous substrate was formed by sintering the α-Al_2O_3 particles and had the average pore diameter of 85 nm and the porosity of 35% and the thickness of 1 mm, the carbon paper was employed in this work to function as the porous substrate. As known, the carbon paper has been widely used in proton exchange membrane fuel cells as the gas diffusion layer, which has good stability and gas permeability [31]. Hence, the carbon paper was used as the porous substrate for the gas permeation and supporting the photocatalyst. In this work, the employed carbon paper (Toray TGPH 090) had the average pore size with the micrometer scale and the porosity of 78% and 0.28 mm in thickness. Clearly, the increased pore size and porosity and the reduced thickness are able to greatly improve the gas permeability. The formation of the composite photocatalytic membrane is illustrated in Fig. 1a. As shown, a porous TiO_2 layer was coated onto the carbon paper. Then the other side of the carbon paper without the photocatalyst layer was treated by PTFE to ensure the hydrophobicity of the developed composite photocatalytic membrane, which facilitated the separation of the gas/liquid phases. The detailed fabrication procedure of this membrane is as follows. The first step was the preparation of the TiO_2 colloid. 6 g TiO_2 nanoparticles (Aeroxide P25, Acros Organics, Belgium) and 0.2 mL acetylacetone were dissolved in 60 mL distilled water and stirred. Then 0.2 mL Triton X-100 (Trition X-100, Sigma Aldrich, USA) and 1.2 g polyethylene glycol were added into the mixture and continuously stirred for over 12 hours to form the TiO_2 colloid. The second step was the spray coating of the TiO_2 colloid on the carbon paper. For better spreading on the substrate, the prepared TiO_2 colloid was diluted with ethanol by the volume ratio of

1:1 before the spray coating. A carbon paper with the dimension of 4.0 cm × 2.0 cm was covered by adhesive tape with the exposed central zone of 1.0 cm × 1.0 cm=1.0 cm^2. The prepared TiO_2 colloid was then spray coated onto the exposed zone of the carbon paper. After finishing the spray coating, the adhesive tape was removed and the TiO_2 coated carbon paper was calcined at 550 ^oC for 2 hours to form a TiO_2 coated carbon paper with the catalyst loading of about 2.0 mg/cm^2. In the final step, the PTFE emulsion (PTFE 60% emulsion, Shanghai Hesen, China) was spray coated on the uncoated side of the carbon paper and heated at 350 ^oC for 30 minutes to improve its hydrophobicity. The total loading of the coated PTFE was nearly 1.0 mg/cm^2. By doing this way, the TiO_2/carbon paper composite photocatalytic membrane was finally achieved.

The prepared membrane was characterized by the scanning electron microscope (SEM) and the results are shown in Figs. 2a and 2b. It can be seen that a uniform porous TiO_2 layer was formed on the carbon paper and the thickness of this layer was about 15 μm. To characterize the hydrophobicity of the membrane, a water droplet was dipped onto the PTFE coated side of the composite photocatalytic membrane and the contact angle was measured by the image technique. As shown in Fig. 3, the contact angle of the PTFE treated surface of the carbon paper was about 139^o, indicating the hydrophobic surface of the membrane was formed to ensure efficient separation of the gas/liquid phases.

2.2 Optofludic membrane microreactor fabrication

As illustrated in Fig. 4a, the optofluidic membrane microreactor was formed by sandwiching two PDMS (Polydimethysiloxane) covers and prepared composite

photocatalytic membrane. A reaction chamber (1 cm × 1 cm × 120 μm) and a membrane supporting chamber (4 cm × 2 cm × 160 μm) were fabricated on both the PDMS covers. The standard SU-8 lithography was used to fabricate the mold. Double-exposure process was carried out to build the two-level terrace shaped SU-8 mold. In this process, the membrane supporting chamber was firstly manufactured. 3.35 g SU-8 photoresist (SU-8 photoresist, Gersteltec Sarl, Switzerland) was spin-coated on the silicon wafer with the rotating speed of 1200 rpm for 60 s to form a layer with the thickness of 160 μm and then heated with the temperature from 65 ^{o}C to 95 ^{o}C by the step increase of 10 ^{o}C. Each temperature step stayed for 15 min. SU-8 photoresist was then exposed under the UV irradiation for 50 s covered by the mask of the membrane supporting chamber. After exposure, the photoresist along with the wafer was heated again, which followed the previous heating procedure to form the membrane supporting chamber. In the second stage, a reaction chamber over the membrane supporting chamber was fabricated. 2.17 g SU-8 photoresist was spin-coated on the previously cured photoresist with the rotating speed of 1200 rpm for 50 s and the thickness of 120 μm and then heated with the same heating procedure. After the same UV exposure with covered mask of the reaction chamber, the silicon wafer along with the SU-8 photoresist was immersed in the developer for 20 min. The remaining developer was then removed by purging nitrogen to form the mold. The PDMS was subsequently poured on the mold and cured, by which two same PDMS covers were fabricated. With these two PDMS covers and the prepared composite photocatalytic membrane, the optofluidic membrane microreactor could be formed by sandwiching these three components with the membrane in the middle. Meanwhile, uncured PDMS was utilized to seal the microreactor to prevent the leakage between covers and the photocatalytic membrane. The assembled microreactor was heated at

95 ^{o}C for 30 minutes at last. The image of the fabricated optofluidic membrane microreactor is shown in Fig. 4b. The dimensions of the reaction chambers for both gas and liquid phases were 1 cm × 1 cm × 120 μm, which corresponded to the volume of 12 μL.

2.3 Experimental setup

In this study, methylene blue (MB) was used as simulated wastewater to evaluate the degradation performance of the optofluidic membrane microreactor under the UV irradiation of 365 nm. The experimental system is illustrated in Fig. 5a. The MB solution was introduced into the liquid reaction chamber using a syringe pump (Harvard Pump 33, Harvard Apparatus, USA). An ozonator (CH-ZTW6G, ChuangHuan, China) was used to generate the ozone and oxygen mixed gas with a constant ozone concentration of 3 ppm. The flow rate of the generated gas was controlled by a gas flowmeter before flowing into the gas reaction chamber. During the experiments, a tunable UV-LED lamp (MXGain-LAB20A, Machine Optoelectronic Technology, China) was projected to the photocatalyst layer through the liquid reaction chamber to actuate the photocatalytic ozonation. The working principle of this optofluidic membrane microreactor is illustrated in Fig. 5b. The ozone gas and MB solution flowed into the gas and liquid reaction chambers, respectively. Because of the composite photocatalytic membrane, they were separated to eliminate the formation of the gas bubbles or slugs in the liquid reaction chamber. The ozone gas was directly transported through the membrane to the photocatalyst layer to complete the photocatalytic ozonation upon illumination. Such operation mode could greatly decrease the mass transfer resistance and enhance the light transport. The liquid products were also collected and subsequently analyzed by an

UV-visible spectrophotometer (TU-1901, Persee) at a wavelength of 664 nm corresponding to the absorbance peak of MB and an ion chromatography (IC, ICS-5000, Thermo Fisher, USA). Each experiment was repeated for at least three times.

3. Results and Discussion

3.1 Performance evaluation

To evaluate the performance of the developed optofluidic membrane microreactor, the MB degradation performances of the photocatalysis, oznonation and photocatalytic ozonation under different liquid flow rates were tested. The photocatalysis, oznonation and photocatalytic ozonation represented the MB degradation only by the UV irradiation with the gas reaction chamber supplied by the inert gas of nitrogen, and only by ozonation without the UV irradiation, and simultaneously by the UV irradiation and ozonation, which were termed as UV, Ozonation and UV+Ozonation, respectively. In the UV degradation, the supply of nitrogen to the gas reaction chamber was to eliminate the possible effect of the oxygen in air to ensure the sole photocatalysis for wastewater treatment. Hence, N_2 was continuously pumped into the gas reaction chamber with the flow rate of 2 mL/min and the light intensity was kept at 7.5 mW/cm^2. In the case of sole ozonation degradation, the ozone gas flow rate was kept at 2 mL/min without the UV irradiation. For the photocatalytic ozonation, the ozone gas flow rate was maintained at 2 mL/min and the light intensity was kept at 7.5 mW/cm^2. The MB concentration was maintained at 3×10^{-5} M. The liquid flow rate ranged from 29.1 μL/min to 145.5 μL/min, which corresponded to the residence times of 25 s, 20 s, 15 s, 10 s and 5 s, respectively.

Fig. 6a compares the degradation efficiencies of three different degradation methods by the optofluidic membrane microreactor under various liquid residence times. It is seen that the UV+Ozonation always yielded the highest degradation efficiency among these three degradation methods. As shown, when the liquid residence time was 15 s, the degradation efficiency of the UV+Ozonation reached 79.6%, which was almost twice of the UV and Ozonation. When the residence time was increased to 25 s, the degradation efficiency of the UV+Ozonation was obtained with 95.2%, while the degradation efficiencies were 48.7% and 74.6% for the UV and Ozonation, respectively. The degradation efficiency of the UV+Ozonation was almost 40% higher than the results of Li et al. [28] and two times higher than the results of Aran et al. [30]. The enhancement was clearly attributed to the novel optofluidic membrane microreactor design to realize the photocatalytic ozonation, which could maximize the synergistic effects of phtocatalysis and ozonation. First of all, the use of the composite photocatalytic membrane with high gas permeability allows ozone and oxygen to be able to efficiently transport through the membrane to the photocatalyst layer, eliminating the mass transfer resistances associated with the gas/liquid interface and liquid film encountered in conventional photocatalytic ozonation. Secondly, the efficiently-transported oxygen resulting from this novel design can function as the electron capturer to generate more oxidizing radicals, which enhances the MB degradation. Thirdly, the efficiently-transported ozone can function as both the electron capturer and powerful oxidant, which further enhances the degradation performance. As a result, the developed optofluidic membrane microreactor exhibited the best degradation performance with the photocatalytic ozonation. This fact also demonstrates the feasibility and superiority of the optofluidic membrane microreactor for wastewater treatment by the photocatalytic ozonation.

In addition, it can be seen that for all cases, the degradation efficiency increased with increasing the residence time. It is easy to understand that an increase in the residence time allowed for more time for MB to be degraded. More ozone could transport through the membrane and be dissolved in the liquid phase instead of washing away. As a result, MB could be more efficiently degraded as the residence time was increased, leading to the improvement in the degradation efficiency for all cases. In addition, it was found that the degradation efficiency of the UV was higher than that of the Ozonation at small residence time and then became lower than the Ozonation at large residence time. The difference between them became more obvious with the residence time further increasing. This might be due to the fact that small residence time caused the permeated ozone to be easily washed away by the coming fluid. In this case, MB could not be efficiently oxidized by the ozone, thus lowering the degradation efficiency. However, this problem was not encountered in the UV. Therefore, the UV yielded better performance than did the Ozonation at small residence time. As the residence time increased, more ozone could be involved into the ozonation, thereby resulting in higher degradation efficiency than that of the UV.

To further gain insight into the improved performance with the optofluidic membrane microreactor for the wastewater treatment by the photocatalytic ozonation, the chemical reaction rate constants with these three degradation methods under different flow rates were also calculated. The reaction rate constants *k* for each case could be calculated by the following equation [32]:

$$k = -\frac{\ln(1-x)}{t} \tag{1}$$

where x is the degradation efficiency and t is the residence time. As can be seen from Fig. 6b, the reaction rate constant of the UV+Ozonation was about twice higher than the UV and Ozonation. Increased reaction rate constant greatly enhanced the photocatalytic ozonation, leading to the best degradation efficiency. Besides, it can also be seen that the k of the UV was higher than that of the Ozonation when the residence time was 5 s. As the residence time increased, the k of the UV gradually decreased. At the residence time of 10 s, it has become lower than that of the Ozonation. This behavior was consistent with the measured degradation efficiency. It is also interesting to find that the reaction rate constants of the UV+Ozonation and Ozonation were slowly increased as the residence time increased, which was converse to the variation trend of the UV. The reason leading to this phenomenon is presented as follows. Generally, the reaction rate constant k depends on the intrinsic reaction rate constant and mass transfer efficiency. Low residence time means high liquid flow rate. For the UV, increasing the liquid flow rate can enhance the mass transport of MB, leading to an improvement in the reaction rate constant with increasing the residence time. However, this is not the case for the Ozonation and UV+Ozonation. Although the increase of the liquid flow rate can enhance the mass transport of MB, the ozone is also easily washed away by the coming fluid instead of being involved in the reaction. Besides, the increase of the liquid flow rate can also dilute the dissolved ozone. Under such a circumstance, the concentrations of the oxidizing reagents become lower. Therefore, the reaction rate constants of the Ozonation and UV+Ozonation decreased with increasing the flow rate as a result of the lowered concentration of the oxidizing reagents.

In this work, the products of the UV, Ozonation and UV+Ozonation were also analyzed by IC. As illustrated in Fig. 7a, the MB molecule contains sulphur atom. The complete oxidation of MB can produce SO_4^{2-} [33]. Hence, the concentration of SO_4^{2-} in the products can be used as the representative to reflect the completion of the MB degradation. The results are shown in Fig. 7b. As seen, the SO_4^{2-} concentration increased with the residence time for all cases. This is because large residence time allowed MB to be more efficiently degraded in the microreactor, leading to an increase in the SO_4^{2-} concentration. It is implied that increasing the residence time cannot only improve the degradation efficiency but also make the degradation more complete. In addition, it can be seen that at low residence time of 5 s, the SO_4^{2-} concentration of the UV was 0.25 mg/L, which was higher than 0.20 mg/L of the Ozonation. It is indicated that small residence time resulted in much more ozone to be washed away. The lowered reagent concentration was unable to completely oxidize MB, lowering the SO_4^{2-} concentration. Increasing the residence time allowed more ozone to be involved in the reaction so that the SO_4^{2-} concentration of the Ozonation became higher than that of the UV. These results were consistent with the measured degradation efficiencies. More importantly, the SO_4^{2-} concentration of the UV+Ozonation was always much higher than those of the UV and Ozonation. For example, at the residence time of 15 s, the SO_4^{2-} concentration of the UV+Ozonation was 0.93 mg/L, which was almost triple higher than the 0.30 mg/L of the UV and 0.31 mg/L of the Ozonation. This is clearly due to the synergistic effect of the photocatalysis and ozonation enhanced by this new microreactor, making the degradation more complete and thereby yielding higher SO_4^{2-} concentration. The

above results reveal that the developed optofluidic membrane microreactor for the wastewater treatment by the photocatalytic ozonzation cannot only yield high degradation efficiency but also make the MB degradation more complete.

3.2 Effect of the light intensity

For the photocatalytic ozonation, the light intensity plays an important role in the MB degradation. Hence, the influence of the light intensity on the degradation performance of the optofluidic membrane microreactor was also investigated in this work. To do this, the ozone gas flow rate was kept 2 mL/min and the MB concentration was remained at 3×10^{-5} M. The light intensity ranged from 5, 7.5 to 10 mW/cm^2, while the residence time ranged from 5 to 15 s. The variations of the degradation efficiency with the light intensity and residence time are shown in Fig. 8. As seen, at the residence time of 5 s, the degradation efficiency was 21.9% under the light intensity of 5 mW/cm^2. As the light intensity increased to 7.5 and 10 mW/cm^2, the degradation efficiency boosted to 38.8% and 78.8%, respectively. In addition, as the residence time increased to 15 s, the degradation efficiency was increased to 60.1%, 79.6% and 98.3% for the light intensities of 5, 7.5 and 10 mW/cm^2, respectively. It is clear that the increase of the residence time allowed more ozone to stay in the microreactor, leading to the increased concentration of the oxidizing reagents. On the other hand, MB could have more time to take part in the reactions. Both positive effects enhanced the MB degradation so that high degradation efficiency could be yielded at large residence time for all cases. Regarding the light intensity, increasing the light intensity resulted in more electron-hole pairs to be excited. As a result, the photocatalytic reaction could be greatly enhanced. Moreover, the supplied ozone, which acted as the electron capturer and oxidant, could further

intensify this process. In this case, the degradation efficiency of the UV+Ozonation was improved with increasing the light intensity. In particular, with the assistance of the supplied ozone, the photocatalysis can be highly enhanced at large light intensity. The synergistic effect of the photocatalysis and ozonation became more significant. Accordingly, the improvement in the degradation efficiency at large light intensity was stronger than that at low light intensity. In summary, the increase of the light intensity can greatly enhance the synergistic effect of the photocatalysis and ozonation by this type of new microreactor, leading to the improvement in the degradation efficiency.

3.4 Effect of the MB concentration

Since the MB concentration is another important factor affecting the performance of the optofluidic membrane microreactor for real applications, the effect of the MB concentration on the degradation performance was also studied in this work. In this measurement, the MB concentration ranged from 3×10^{-5} to 9×10^{-5} M, while the light intensity was kept at 7.5 mW/cm^2 and the gas flow rate was kept at 2 mL/min and the residence time ranged from 5 to 15 s. The results are shown in Fig. 9. At the residence time of 5 s, the degradation efficiencies were 12.4%, 29.0% and 38.8% corresponding to the MB concentration of 9×10^{-5}, 6×10^{-5} and 3×10^{-5} M, respectively. At large residence time of 15 s, the degradation efficiencies were increased to 49.7%, 67.5% and 79.6%. Obviously, although the increase of the MB concentration could enhance the mass transport of MB due to the increased concentration gradient between the bulk and photocatalytic membrane, the degradation efficiency still dropped as the MB concentration increased. The decrease of the degradation performance was mainly attributed to the following reasons. First

of all, the increase of the MB concentration increased the load to the developed optofluidic membrane microreactor. However, the degrading capability of the microreactor was limited so that high MB concentration led to low degradation efficiency. Second, high MB concentration could cause more intermediates to be generated at the same time. In this case, more active cites of the photocatalysts were covered by those intermediates. As a consequence, the reactions between MB and oxidizing reagents including light induced holes and hydroxyl radicals were blocked, leading to the low degradation efficiency. Third, high MB concentration increased the photon transfer resistance resulting from the optical attenuation, which weakened the generation of the light induced electron-hole pairs and thereby further lowered the degradation efficiency. However, even under high MB concentration of 9×10^{-5} M, the developed microreactor still showed a relatively high degradation efficiency of 49.7% with a short residence time 15 s. This fact indicates that the optofluidic membrane reactor developed in this work possesses a broad operation range.

4. Conclusions

In this work, a novel optofluidic membrane microreactor was developed for the wastewater treatment by the photocatalytic ozonation. To this end, a TiO_2/carbon paper composite photocatalytic membrane was prepared by coating TiO_2 onto the carbon paper and followed by the PTFE treatment of the other side of the carbon paper. Such design can enhance the photon and mass transport because of large surface-area-to-volume ratio. Especially, the ozone transport issue associated with the gas/liquid interface and liquid film in conventional photocatalytic ozonation technologies can be efficiently addressed. The synergistic effect of the photocatalysis and ozonation can thus be greatly intensified. The performance of the developed

microreactor was evaluated by the MB degradation and the product of SO_4^{2-} was analyzed by the IC. The experimental results indicated that because of the above mentioned advantages, not only the degradation efficiency of the photocatalytic ozonation was greatly improved, but also the MB degradation became more complete as compared to the conventional photocatalysis and ozonation technologies. Effects of the operation parameters including the liquid flow rate, light intensity and MB concentration were also investigated to assess the degradation performance characteristics of the developed membrane microreactor. It was shown that increasing the residence time could improve the degradation efficiency because the reaction time was increased for MB and more ozone was involved in the reactions instead of washing away. High light intensity could generate more electron-hole pairs for the photocatalysis and intensify the synergistic effect of the photocatalysis and ozonation, leading to the improvement in the degradation efficiency. Besides, it was also shown that despite the mass transport of MB was enhanced with high MB concentration, the developed optofluidic membrane microreactor still yielded better performance at low MB concentration because of the limited capability of the developed microreactor, more intermediates and optical attenuation resulting from high MB concentration. This work fully demonstrates the feasibility and superiority of the developed optofluidic membrane microreactor for the wastewater treatment by the photocatalytic ozonation. It should be pointed out that the application of the developed optofluidic membrane microreactor is still difficult for industrial wastewater treatment by the photocatalytic ozonation because of the limited throughput based on the current device. One of the strategies to overcome this limitation can be directed to the integration of multiple microreactors to form a module and then adequate selection

and arrangement of the modules to improve the throughput, which requires further investigation before its widespread commercialization.

Acknowledgements

The authors gratefully acknowledge the financial supports of the National Natural Science Foundation of China (No. 51222603, No. 51276208, No. 51325602 and No. 51576021), Specialized Research Fund for the Doctoral Program of Higher Education of China (No. 20120191110010) and the Program for New Century Excellent Talents in University (NCET-12-0591).

References

[1] Kornaros M.; Lyberatos G. Biological treatment of wastewaters from a dye manufacturing company using a trickling filter. *J. Hazard. Mater.* **2006**, 136, 95-102.

[2] Ledakowicz S.; Solecka M.; Zylla R. Biodegradation, decolourisation and detoxification of textile wastewater enhanced by advanced oxidation processes. *J. Biotechnol.* **2001**, 8, 175-184.

[3] Kang S. F.; Liao C. H.; Chen M. C. Pre-oxidation and coagulation of textile wastewater by the Fenton process. *Chemosphere* **2002**, 46, 923–928.

[4] Szpyrkowicz L.; Juzzolino C.; Kaul S. N. A comparative study on oxidation of disperse dyes by electrochemical process, ozone, hypochlorite and Fenton reagent. *Water Res.* **2001**, 35, 2129-2136.

[5] Tan B. H.; Teng T. T.; Omar A. K. M. Removal of dyes and industrial dye wastes by magnesium chloride. *Water Res.* **2000**, 34, 597-601.

[6] Lachheb H.; Puzenat E.; Houas A. Photocatalytic degradation of various types of dyes (Alizarin S, Crocein Orange G, Methyl Red, Congo Red, Methylene Blue) in water by UV-irradiated titania. *Appl. Catal. B-Environ.* **2002**, 39, 75-90.

[7] Khataee A. R.; Kasiri M. B. Photocatalytic degradation of organic dyes in the presence of nanostructured titanium dioxide: influence of the chemical structure of dyes. *J. Mol. Catal. A-Chem.* **2010**, 328, 8-26.

[8] Chowdhury S.; Balasubramanian R. Graphene/semiconductor nanocomposites (GSNs) for heterogeneous photocatalytic decolorization of wastewaters contaminated with synthetic dyes: a review. *Appl. Catal. B-Environ*. **2014**, 160, 307-324.

[9] Dong S.; Feng J.; Fan M. Recent developments in heterogeneous photocatalytic water treatment using visible light-responsive photocatalysts: a review. *RSC Adv*. **2015**, 5, 14610-14630.

[10] Wang C. C.; Li J. R.; Lv X. L. Photocatalytic organic pollutants degradation in metal–organic frameworks. *Energy Environ. Sci*. **2014**, 7, 2831-2867.

[11] Henschel D. B. Cost analysis of activated carbon versus photocatalytic oxidation for removing organic compounds from indoor air. *J. Air Waste Manag. Assoc*. **1998**, 48, 985–994.

[12] Gupta V. K.; Jain R.; Nayak A. Removal of the hazardous dye—tartrazine by photodegradation on titanium dioxide surface. *Mat. Sci. Eng. C-Mater*. **2011**, 31, 1062-1067.

[13] Sakthivel S.; Neppolian B.; Shankar M. V. Solar photocatalytic degradation of azo dye: comparison of photocatalytic efficiency of ZnO and TiO_2. *Sol. Energy Mater. Sol. Cells* **2003**, 77, 65-82.

[14] Keller V.; Bernhardt P.; Garin F. Photocatalytic oxidation of butyl acetate in vapor phase on TiO_2, Pt/TiO_2 and WO_3/TiO_2 catalysts. *J. Catal.* **2003**, 215, 129-138.

[15] Zhu H.; Jiang R.; Xiao L. Photocatalytic decolorization and degradation of Congo Red on innovative crosslinked chitosan/nano-CdS composite catalyst under visible light irradiation. *J. Hazard. Mater.* **2009**, 169, 933-940.

[16] Štengl V.; Velická J.; Maríková M. New generation photocatalysts: how tungsten influences the nanostructure and photocatalytic activity of TiO_2 in the UV and visible regions. *ACS Appl. Mater. Interfaces* **2011**, 3, 4014-4023.

[17] Mehrjouei M.; Müller S.; Möller D. A review on photocatalytic ozonation used for the treatment of water and wastewater. *Chem. Eng. J.* **2015**, 263, 209-219.

[18] Mehrjouei M.; Müller S.; Möller D. Synergistic effect of the combination of immobilized TiO_2, UVA and ozone on the decomposition of dichloroacetic acid. *J. Environ. Sci. Heal. A* **2012**, 47, 1073-1081.

[19] Beduk F.; Aydin M. E.; Ozcan S. Degradation of malathion and parathion by ozonation, photolytic ozonation, and heterogeneous catalytic ozonation processes. *Clean-Soil Air Water* **2012**, 40, 179-187.

[20] Hur J. S.; Oh S. O.; Lim K. M. Novel effects of TiO_2 photocatalytic ozonation on control of postharvest fungal spoilage of kiwifruit. *Postharvest Biol. Technol.* **2005**, 35, 109-113.

[21] Fathinia M.; Khataee A. Photocatalytic ozonation of phenazopyridine using TiO_2 nanoparticles coated on ceramic plates: mechanistic studies, degradation intermediates and ecotoxicological assessments. *Appl. Catal. A-Gen.* **2015**, 491, 136-154.

[22] Maddila S.; Lavanya P.; Jonnalagadda S. B. Degradation, mineralization of bromoxynil pesticide by heterogeneous photocatalytic ozonation. *J. Ind. Eng.* **2015**, 24, 333-341.

[23] Wang N.; Zhang X.; Wang Y. Microfluidic reactors for photocatalytic water purification. *Lab Chip* **2014**, 14, 1074-1082.

[24] Erickson D.; Sinton D.; Psaltis D. Optofluidics for energy applications. *Nat. Photonics* **2011**, 5, 583-590.

[25] Wang N.; Zhang X.; Chen B. Microfluidic photoelectrocatalytic reactors for water purification with an integrated visible-light source. *Lab Chip* **2012**, 12, 3983-3990.

[26] Li L.; Wang G.; Chen R. Optofluidics based micro-photocatalytic fuel cell for efficient wastewater treatment and electricity generation. *Lab Chip* **2014**, 14, 3368-3375.

[27] Hashemi S. M. H.; Choi J. W.; Psaltis D. Solar thermal harvesting for enhanced photocatalytic reactions. *Phys. Chem. Chem. Phys.* **2014**, 16, 5137-5141.

[28] Li L.; Chen R.; Zhu X. Optofluidic microreactors with TiO_2-coated fiberglass. *ACS Appl. Mater. Interfaces* **2013**, 5, 12548-12553.

[29] Lei L.; Wang N.; Zhang X. M. Optofluidic planar reactors for photocatalytic water treatment using solar energy. *Biomicrofluidics* **2010**, 4, 043004.

[30] Aran H. C.; Salamon D.; Rijnaarts T. Porous photocatalytic membrane microreactor (P2M2): a new reactor concept for photochemistry. *J. Photoch Photobio A* **2011**, 225, 36-41.

[31] Lim C.; Wang C. Y. Effects of hydrophobic polymer content in GDL on power performance of a PEM fuel cell. *Electrochim. Acta* **2004**, 49, 4149-4156.

[32] Lin H.; Valsaraj K. T. Development of an optical fiber monolith reactor for photocatalytic wastewater treatment. *J. Appl. Electrochem.* **2005**, 35, 699-708.

[33] Houas A.; Lachheb H.; Ksibi M. Photocatalytic degradation pathway of methylene blue in water. *Appl. Catal. B-Environ.* **2001**, 31, 145-157.

Figure captions

Figure 1 Illustration of the TiO_2/carbon paper composite photocatalytic membrane.

Figure 2 SEM images of the TiO_2/carbon paper composite photocatalytic membrane, (a) top view and (b) cross-sectional view.

Figure 3 Wettability of the carbon paper after the PTFE treatment.

Figure 4 (a) Schematic and (b) Image of the optofluidic membrane microreactor.

Figure 5 Illustrations of (a) the experimental system and (b) the working principle of the optofluidic membrane microreactor.

Figure 6 Comparison of (a) the degradation efficiency and (b) reaction rate constant between the UV, Ozonation and UV+Ozonation under different residence times. Light intensity: 7.5 mW/cm^2, MB concentration: 3×10^{-5} M, Gas flow rate: 2 mL/min.

Figure 7 (a) Molecular structure of methylene blue, and (b) Comparison of the SO_4^{2-} concentration between the UV, Ozonation and UV+Ozonation under different residence times. Light intensity: 7.5 mW/cm^2, MB concentration: 3×10^{-5} M, Gas flow rate: 2 mL/min.

Figure 8 Effect of the light intensity on the degradation efficiency for the UV+Ozonation. MB concentration: 3×10^{-5} M, Gas flow rate: 2 mL/min.

Figure 9 Effect of the MB concentration on the degradation efficiency for the UV+Ozonation. Light intensity: 7.5 mW/cm^2, Gas flow rate: 2 mL/min.

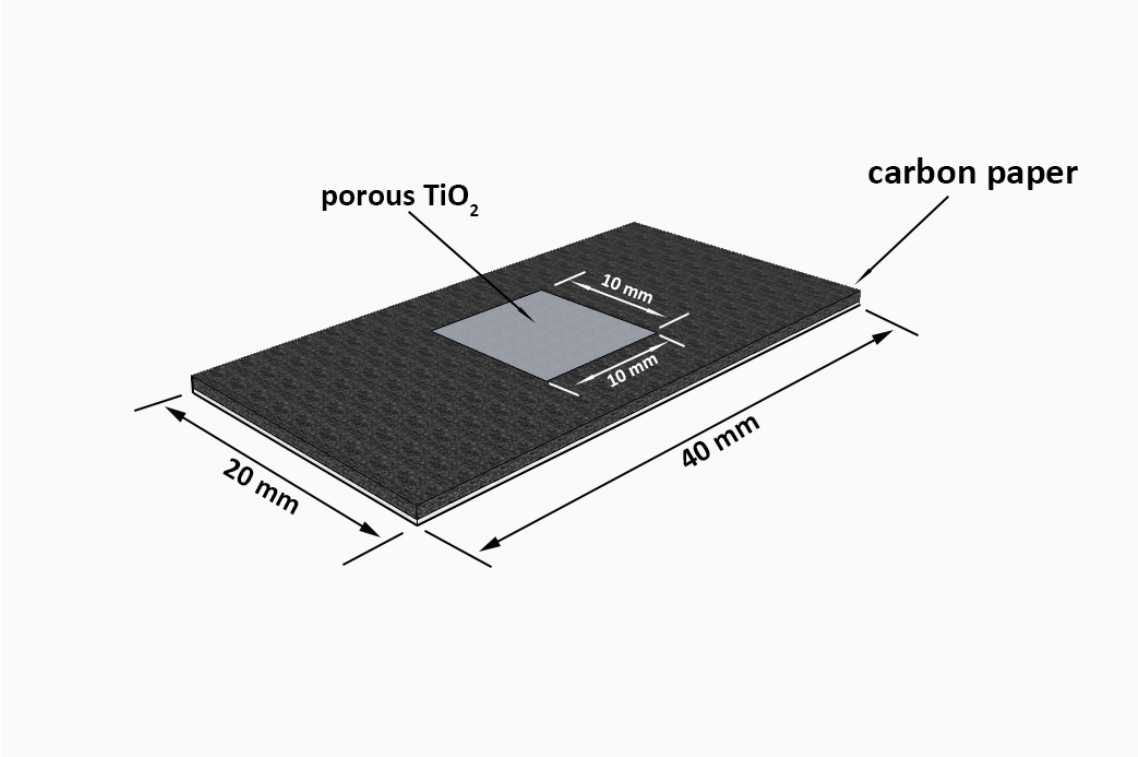

Fig. 1

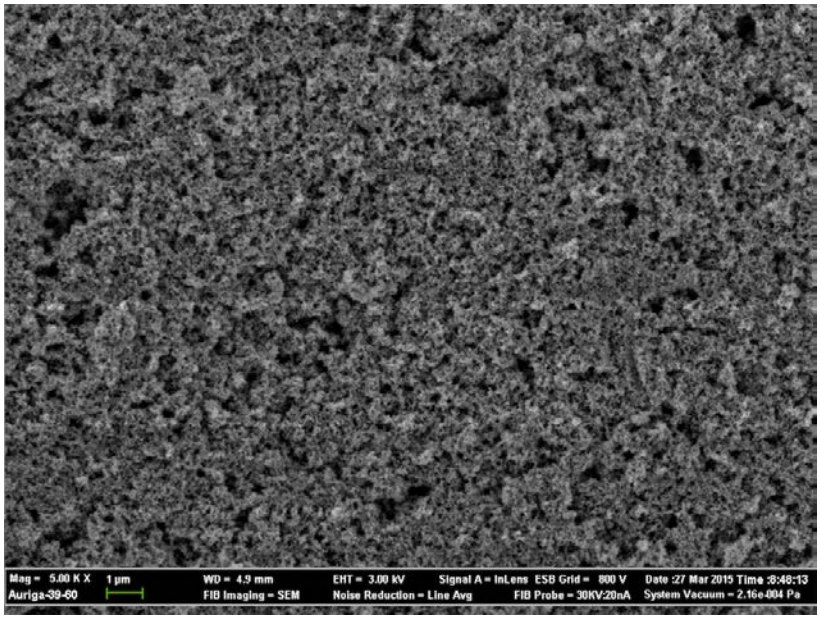
Mag = 5.00 K X 1 µm
Auriga-39-60
WD = 4.9 mm
FIB Imaging = SEM
EHT = 3.00 kV
Noise Reduction = Line Avg
Signal A = InLens ESB Grid = 800 V
FIB Probe = 30KV:20nA
Date :27 Mar 2015 Time :8:48:13
System Vacuum = 2.16e-004 Pa

(a)

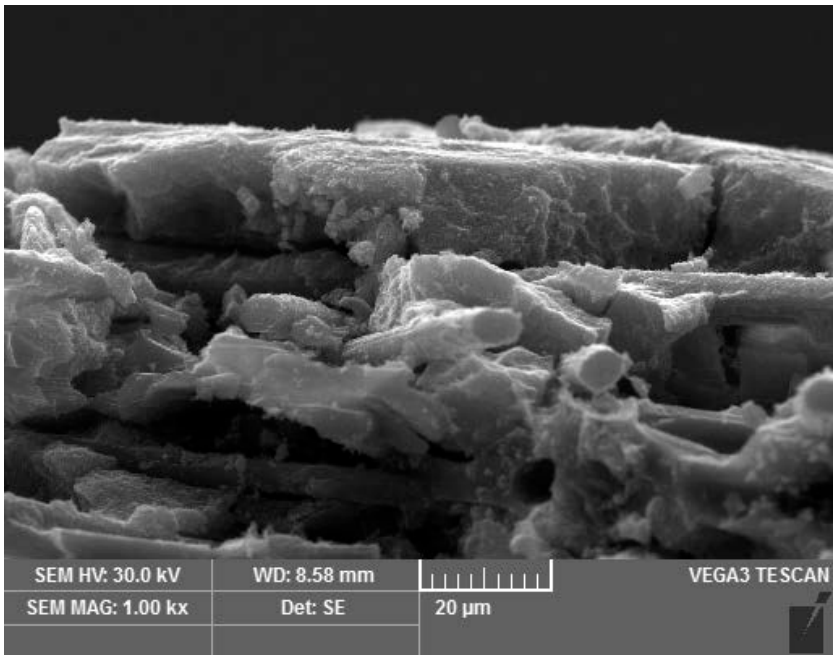
SEM HV: 30.0 kV
WD: 8.58 mm
VEGA3 TESCAN
SEM MAG: 1.00 kx
Det: SE
20 µm

(b)

Fig. 2

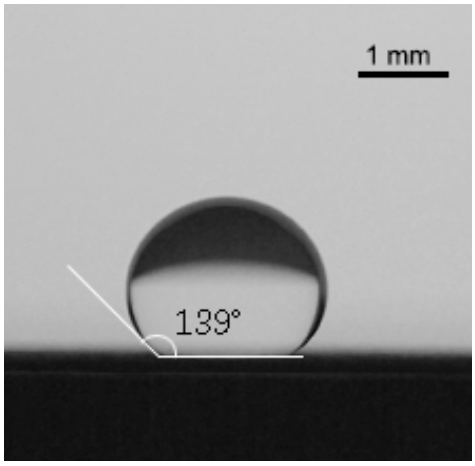

Fig. 3

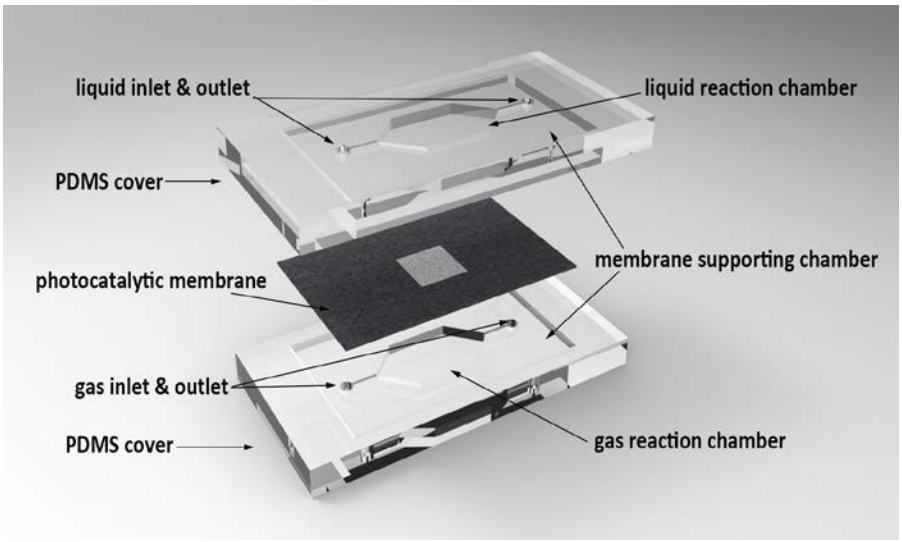
liquid inlet & outlet
liquid reaction chamber
PDMS cover
membrane supporting chamber
photocatalytic membrane
gas inlet & outlet
PDMS cover
gas reaction chamber

(a)

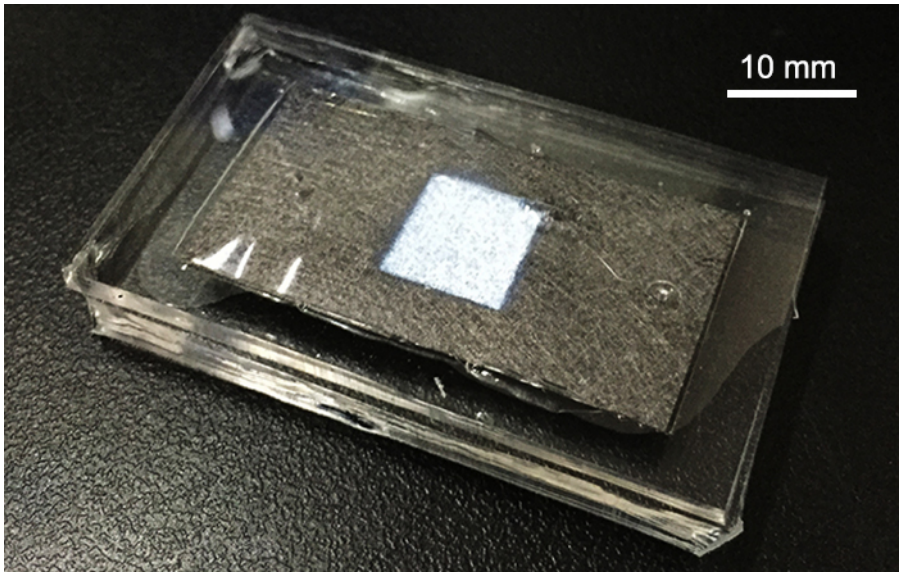
10 mm

(b)

Fig. 4

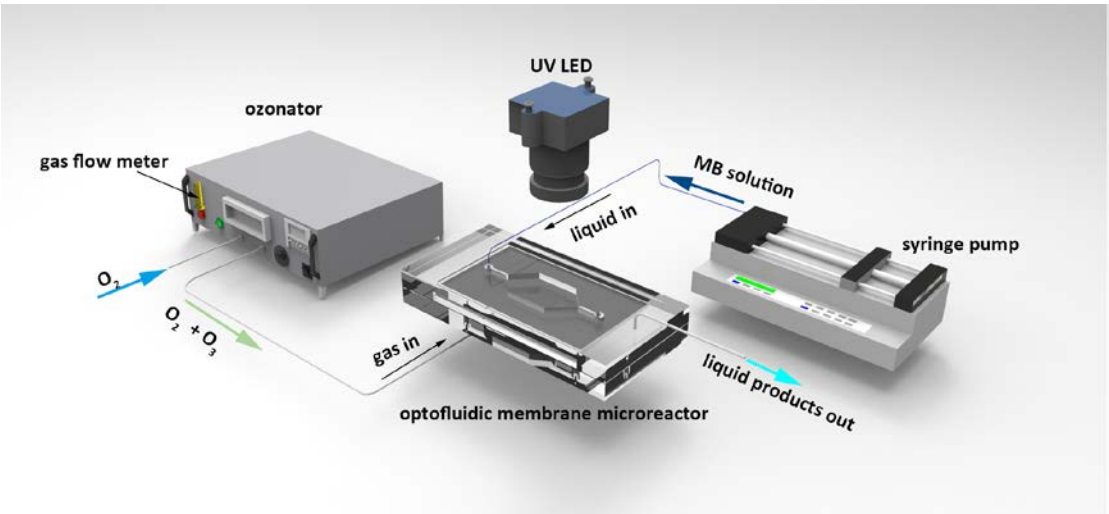
UV LED
ozonator
gas flow meter
MB solution
liquid in
syringe pump
O_2
$O_2 + O_3$
gas in
liquid products out
optofluidic membrane microreactor

(a)

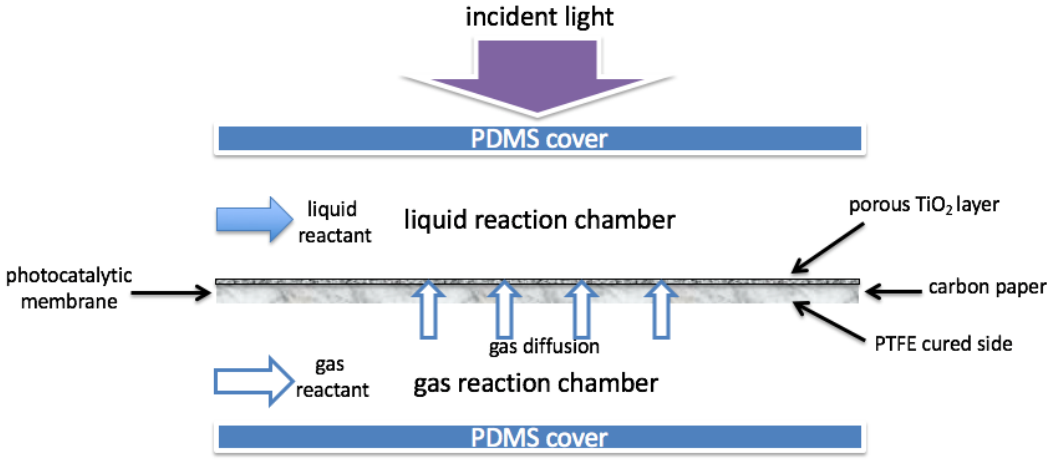
incident light
PDMS cover
liquid reactant
liquid reaction chamber
porous TiO_2 layer
photocatalytic membrane
carbon paper
gas diffusion
PTFE cured side
gas reactant
gas reaction chamber
PDMS cover

(b)

Fig. 5

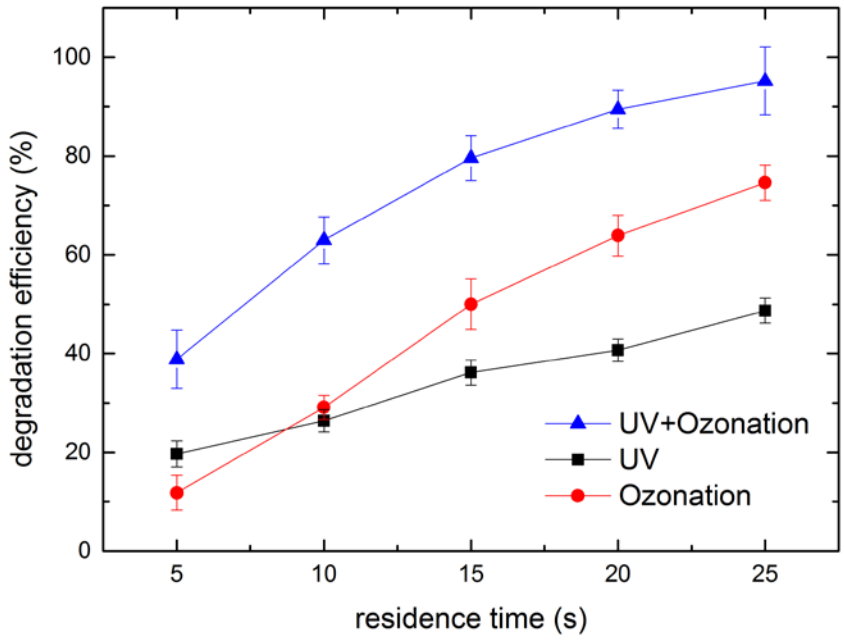
degradation efficiency (%)
residence time (s)
UV+Ozonation
UV
Ozonation

(a)

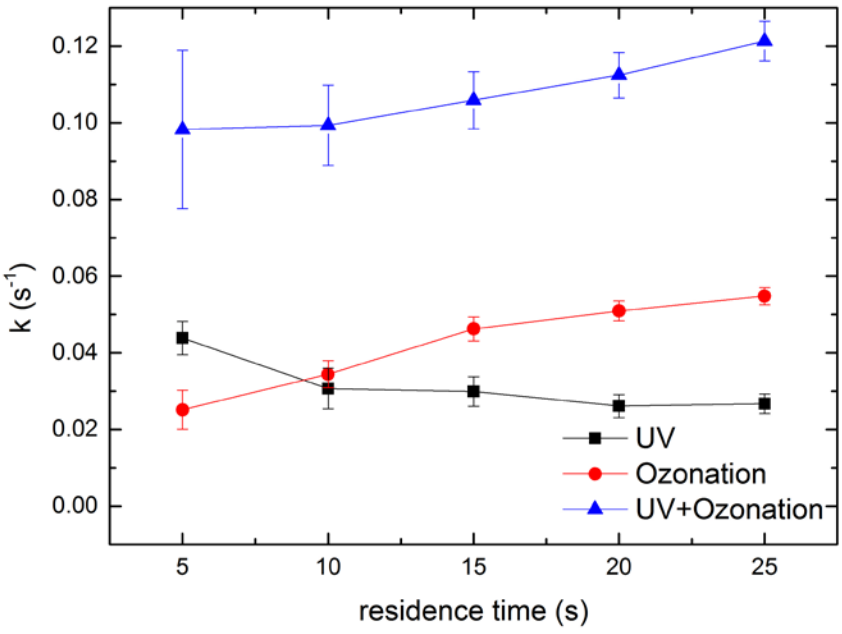
k (s-1)
residence time (s)
UV
Ozonation
UV+Ozonation

(b)

Fig. 6

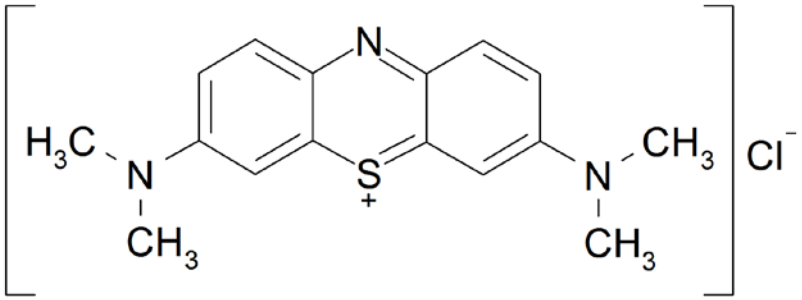
N
H3C
N
CH3
S
+
N
CH3
CH3
Cl-

(a)

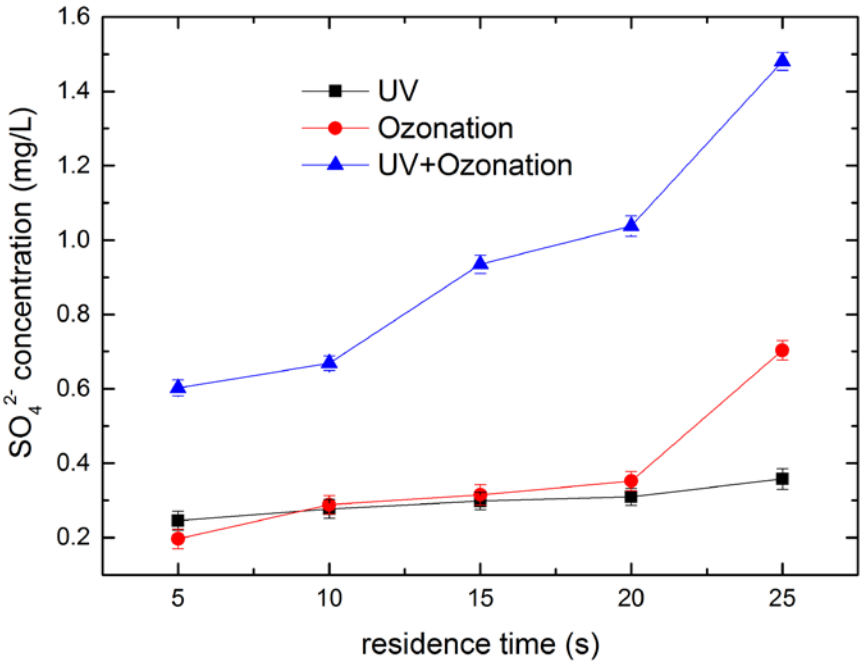
UV
Ozonation
UV+Ozonation
SO4 2- concentration (mg/L)
residence time (s)
1.6
1.4
1.2
1.0
0.8
0.6
0.4
0.2
5
10
15
20
25

(b)

Fig. 7

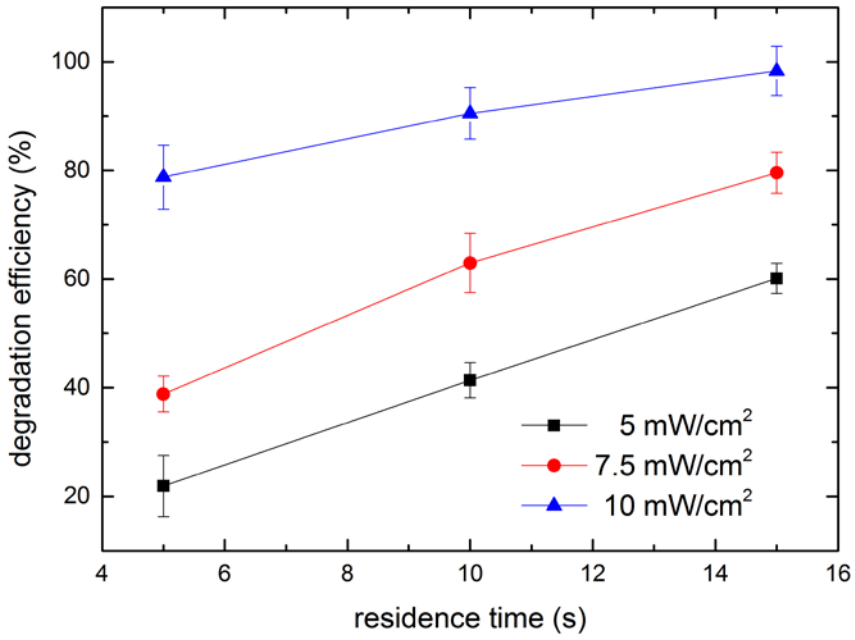
degradation efficiency (%)
100
80
60
40
20
4
6
8
10
12
14
16
residence time (s)
5 mW/cm2
7.5 mW/cm2
10 mW/cm2

Fig. 8

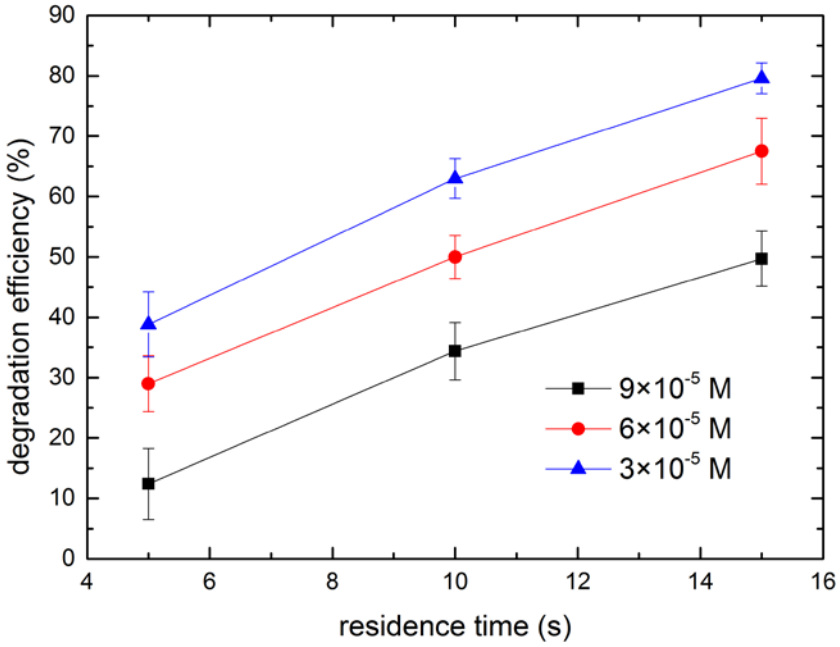
degradation efficiency (%)
residence time (s)
9×10-5 M
6×10-5 M
3×10-5 M
0
10
20
30
40
50
60
70
80
90
4
6
8
10
12
14
16

Fig. 9

Table of Contents